nature
structural &
molecular biology

Telomere end-binding proteins control the formation of G-quadruplex DNA structures *in vivo*

Katrin Paeschke[1,3], Tomas Simonsson[2,3], Jan Postberg[1], Daniela Rhodes[2] & Hans Joachim Lipps[1]

Telomere end-binding proteins (TEBPs) bind to the guanine-rich overhang (G-overhang) of telomeres. Although the DNA binding properties of TEBPs have been investigated *in vitro*, little is known about their functions *in vivo*. Here we use RNA interference to explore *in vivo* functions of two ciliate TEBPs, TEBPα and TEBPβ. Silencing the expression of genes encoding both TEBPs shows that they cooperate to control the formation of an antiparallel guanine quadruplex (G-quadruplex) DNA structure at telomeres *in vivo*. This function seems to depend on the role of TEBPα in attaching telomeres in the nucleus and in recruiting TEBPβ to these sites. *In vitro* DNA binding and footprinting studies confirm the *in vivo* observations and highlight the role of the C terminus of TEBPβ in G-quadruplex formation. We have also found that G-quadruplex formation *in vivo* is regulated by the cell cycle–dependent phosphorylation of TEBPβ.

Telomeres, the protein–DNA complexes at the termini of eukaryotic chromosomes, protect chromosomes from degradation. They prevent the telomeric ends from being recognized as sites of DNA damage, ensure complete replication of the genome and contribute to nuclear architecture[1–3]. Telomeric DNA consists of tandem repeats of a short sequence motif containing a guanine-rich strand which is oriented 5′ to 3′ toward the chromosome terminus. The protrusion of the guanine-rich strand to form a single-stranded G-overhang is a feature conserved from simple eukaryotes to vertebrates[4–6]. Telomeres in the macronucleus of the ciliate protozoan *Stylonychia lemnae* end with a G-overhang consisting of 16 nucleotides (nt), $T_4G_4T_4G_4$ (**Fig. 1a**), which is bound by two TEBPs, TEBPα and TEBPβ. These TEBPs are characterized by the presence of oligonucleotide/oligosaccharide–binding folds (OB folds) that are involved in single-stranded DNA binding[7,8]. Recently it has been discovered that the fission yeast and human Pot1 proteins are structural homologs of TEBPα[9], suggesting conservation in G-overhang binding and protection.

Biochemical and structural studies have shown that TEBPs can form two different complexes at telomeres and that these are likely to have different functions. The 56-kDa TEBPα binds specifically to the telomeric G-overhang[10]. This complex can further homodimerize, as seen in the crystal structure of a TEBPα–T_4G_4 complex[11], suggesting a possible mechanism for telomere-telomere association. The 41-kDa TEBPβ does not bind the telomeric G-overhang by itself, but heterodimerizes with TEBPα in a DNA-dependent manner[12,13]. The crystal structure of the TEBPα-β heterodimer in complex with $G_4T_4G_4$ shows the DNA in an extended single-stranded conformation. The 3′ hydroxyl group of the last guanine is buried deep within the protein complex, suggesting it serves as a telomere cap[14]. Notably in relation to the study presented here, the TEBPβ present in the crystal structure is truncated and lacks the C terminus. *In vitro* studies have suggested that the C terminus of TEBPβ can change the structure of telomeric G-overhangs[15]. Despite detailed knowledge of the way in which TEBPs bind to telomeric DNA *in vitro*, their *in vivo* functions have remained unknown.

Besides having a role in recruiting TEBPs, telomeric G-overhangs can form G-quadruplex DNA structures[16,17] at physiological salt concentrations *in vitro*[18]. Four guanines can adopt a flat, cyclic Hoogsteen hydrogen-bonding arrangement known as the guanine tetrad, in which each guanine serves as both hydrogen bonding acceptor and donor (**Fig. 1b**) and the stacking of guanine tetrads results in G-quadruplex DNA structures (**Fig. 1c**). For instance, two telomeric 3′ $T_4G_4T_4G_4$ overhangs can form hairpins that dimerize to give rise to G-quadruplex DNA structures with antiparallel strands.

G-quadruplex DNA structures have attracted considerable attention because they provide a simple mechanism for telomere-telomere interactions[19] and inhibit telomerase activity *in vitro*[20]. Although there is accumulating *in vitro* evidence for G-quadruplex DNA structures, demonstration of their *in vivo* formation has proven elusive. Recent analyses using specific antibodies have provided the first direct evidence that an antiparallel G-quadruplex DNA structure is present at telomeres in the macronucleus of stichotrichous ciliates *in vivo*[21].

Macronuclear DNA of stichotrichous ciliates consists of small DNA molecules (nanochromosomes), each terminated by telomeres. A single macronucleus of *Stylonychia* contains about 1×10^8 nanochromosomes[3]. Several studies have suggested that the nanochromosomes are assembled into a higher-order structure *in vivo* via their

[1]Institute of Cell Biology, University Witten/Herdecke, Stockumer Strasse 10, 58453 Witten, Germany. [2]Medical Research Council, Laboratory of Molecular Biology, Hills Road, Cambridge CB2 2QH, UK. [3]These authors contributed equally to this work. Correspondence should be addressed to H.J.L. (lipps@uni-wh.de) and D.R. (rhodes@mrc-lmb.cam.ac.uk).

Received 31 May; accepted 3 August; published online 4 September 2005; doi:10.1038/nsmb982

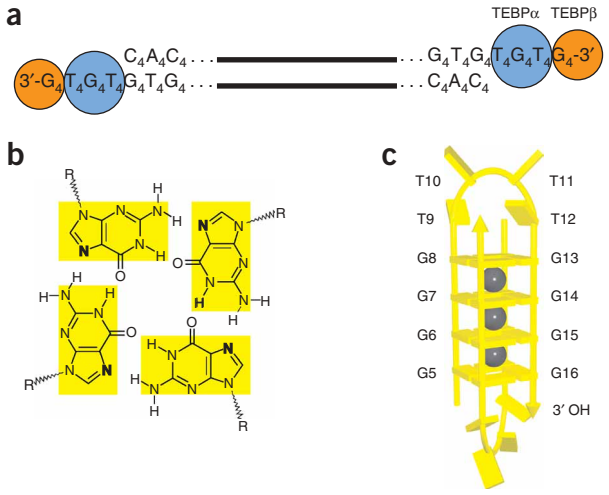

Figure 1 Schematic representation of a macronuclear nanochromosome. (**a**) Each telomeric 3′ overhang binds one TEBPα (blue) and one TEBPβ (orange). (**b**) The hydrogen bonding pattern of guanine tetrads (yellow) uniquely involves the exocyclic amino group N7 (bold). (**c**) Formation of an antiparallel G-quadruplex DNA structure from two G-overhangs. Stabilizing cations are shown as black spheres.

telomeres[22–24]. Analysis of telomere organization has shown that telomeres are attached to a subnuclear structure[25], as has been reported for other eukaryotic cells[26–28]. In a follow-up study, we discovered that telomeres adopt a G-quadruplex DNA structure when attached to a subnuclear structure[29]. Both the attachment of telomeres and the G-quadruplex DNA structure seem to have been resolved during replication[21,25]. Nevertheless, the molecular nature of telomere attachment and the proteins involved in formation of G-quadruplex DNA structures are still unknown.

Here we use RNA interference (RNAi) to silence expression of the TEBP genes, a strategy that for the first time permits analysis of their *in vivo* functions. Our results show that TEBPα and TEBPβ have separate but essential roles in telomere attachment and in the formation and regulation of G-quadruplex DNA structures at telomeres. *In vitro* binding studies pinpoint the precise roles of the TEBPs in the formation of G-quadruplex DNA structures. Furthermore, we find that G-quadruplex formation *in vivo* is regulated by phosphorylation of TEBPβ. These data allow us to propose a model for the way TEBPs modulate telomere structure *in vivo*.

RESULTS

TEBPα attaches telomeres in the nucleus and recruits TEBPβ

We investigated whether the two TEBPs have a role in the attachment of telomeres to a subnuclear structure by using nuclear electroelution[25,30], which is a powerful technique to test whether nuclear components are bound to subnuclear structures *in vivo*. Cells were embedded into low–melting point agarose and permeabilized, and then the DNA was restriction digested in the gel. An electric field was then applied to elute unbound DNA and proteins. Fluorescence *in situ* hybridization (FISH) analysis using a telomeric DNA probe showed that telomeres could not be electroeluted from the macronucleus (**Fig. 2a**,**b**). Similarly, immunolocalization of TEBPα and TEBPβ showed that both were bound to the subnuclear structure *in vivo* (**Fig. 2c–f**). Replication of macronuclear DNA occurs in a morphologically distinct region, the replication band (**Fig. 2a–f**, arrow), and this allowed us to observe the behavior of telomeres and the two TEBPs by light microscopy during replication. In macronuclei that had not been electroeluted, FISH with telomeric probes (**Fig. 2a**) and immunolocalization of TEBPα (**Fig. 2c**) and TEBPβ (**Fig. 2e**) showed a strong staining that colocalized with the replication band. After electroelution, neither telomeres (**Fig. 2b**) nor TEBPs (**Fig. 2d**,**f**) could be detected in the replication band, indicating that neither remained attached to a subnuclear structure.

We next assessed the individual roles of TEBPα and TEBPβ in telomere attachment *in vivo* by silencing their expression. This was achieved by feeding cells with *Escherichia coli* expressing double-stranded (ds) RNA directed against the mRNAs encoding the proteins[31]. As shown by *in situ* antibody staining and western analyses (**Fig. 3a–f**), expression of the TEBP genes was almost completely silenced 4 d after *Stylonychia* were fed with dsRNA-expressing *E. coli*. This phenotype was seen in over 95% of the cells, consistent with an observed decrease in intensity of the respective TEBP bands in western analyses (**Fig. 3**). At this time the cells were fully viable, as shown by the presence of replication bands and dividing cells. Silencing of TEBPα or TEBPβ eventually led to cell death (~14–21 d). After this time telomeres were no longer detectable by Southern analysis and the DNA was degraded and lost from the nucleus (data not shown). This effect was also observed when different regions of the TEBP genes were targeted by RNAi.

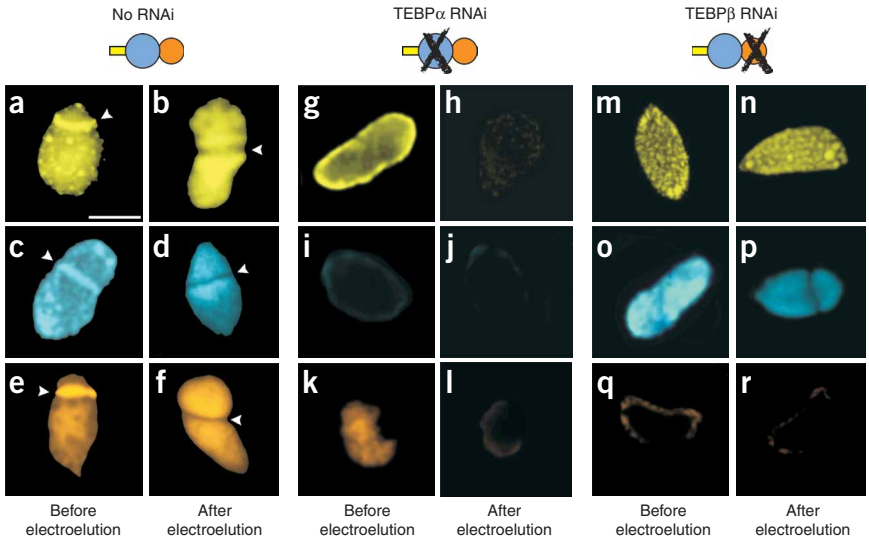

Figure 2 TEBPα attaches telomeres to a subnuclear structure and recruits TEBPβ to the attachment sites. The localization of telomeric DNA was examined by FISH analysis and TEBP localization was examined by *in situ* antibody staining. (**a–r**) *Stylonychia* macronuclei after FISH analysis with telomeric probe (yellow), or after *in situ* antibody staining of TEBPα (blue) or TEBPβ (orange), before or after electroeleution as indicated; arrows, replication band; scale bar represents 10 μm. Schematics show constituents of complexes in the experiments: blue, TEBPα; orange, TEBPβ; crosses, silencing of either TEBPα (**g–l**) or TEBPβ (**m–r**) expression by RNAi.

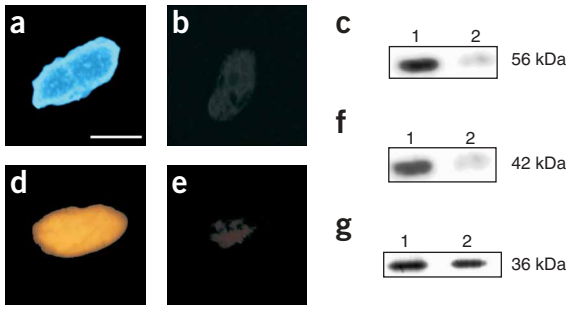

Figure 3 Silencing of TEBPα and TEBPβ gene expression by RNAi. (**a**–**g**) *In situ* antibody staining of the two TEBPs (**a**,**b**,**d**,**e**; coloring as in **Fig. 2**; scale bar represents 10 μm) and western analyses (**c**,**f**,**g**). (**a**,**b**) TEBPα in control cells (**a**) and after silencing (**b**). (**c**) Western blots using antibodies directed against TEBPα in control cells (lane 1) and after silencing TEBPα (lane 2). (**d**,**e**) TEBPβ in control cells (**d**) and after silencing (**e**). (**f**) Western blots using antibodies directed against TEBPβ in control cells (lane 1) and after silencing TEBPβ (lane 2). (**g**) Control western blot using monoclonal antibody 38F3 (EnCor Biotechnology) to fibrillarin/nop1p, after silencing of TEBPα.

In addition, we studied telomere attachment after silencing of either TEBPα or TEBPβ expression using nuclear electroelution. Silencing of TEBPα expression by RNAi for 4 d resulted in the loss of telomere attachment, and telomeres could then be completely electroeluted from the nucleus (**Fig. 2g**,**h**). This was not the result of degradation of telomeric DNA, as shown by FISH analyses of nuclei before electroelution (**Fig. 2g**) and by sequence analyses of telomeric DNA (**Supplementary Tables 1–3** online). Silencing of TEBPα expression (**Fig. 2i**,**j**) followed by electroelution resulted in complete removal of the TEBPβ from the macronucleus (**Fig. 2k**,**l**). In contrast, neither the telomeres (**Fig. 2m**,**n**) nor TEBPα (**Fig. 2o**,**p**) could be electroeluted from the nucleus after silencing of TEBPβ expression (**Fig. 2q**,**r**). These results show that telomere attachment is mediated by TEBPα and that TEBPβ localizes to telomeres through interactions with TEBPα.

Both TEBPs are required for G-quadruplex formation *in vivo*

We asked whether tethering of telomeres in the nucleus is related to the formation of G-quadruplex DNA structures *in vivo*. G-quadruplex DNA structures at macronuclear telomeres *in vivo* were detected using antibodies generated by ribosome display from the Human Combinatorial Antibody Library[21,32] . These antibodies were highly specific, with affinities for telomeric G-quadruplex DNA structures between $K_d = 0.125$ nM and $K_d = 5$ nM. Moreover, they could be used to distinguish between parallel and antiparallel conformations[21]. No staining was obtained with Sty3, an antibody against the parallel G-quadruplex conformation (**Fig. 4a**), providing an essential control showing that the observed G-quadruplex DNA structure was not an artifact that occurred upon antibody binding. Only Sty49, an antibody directed against both G-quadruplex conformations, gave a positive signal (**Fig. 4b**,**c**). Thus, only the antiparallel G-quadruplex DNA structure is present *in vivo*[21]. Staining with Sty49 showed the same focal organization as was observed in FISH analyses using a telomeric probe or after staining with antibodies against TEBPs. Therefore, it is likely that G-quadruplex staining overlaps with telomeres, as concluded earlier[21]. Moreover, the antibodies do not stain the replication band (**Fig. 4b**). As antibodies against B-DNA react strongly with the replication band[33], the absence of staining with antibodies against G-quadruplex DNA cannot be explained by lower accessibility of the DNA in the replication band. From this we conclude that the telomeric G-quadruplex DNA structure is unfolded during replication.

To investigate whether the two TEBPs are involved in the formation of G-quadruplex DNA structures at telomeres, we again silenced their expression silenced by RNAi, but this time we analyzed the effect on telomere structure with the Sty49 antibody. Silencing of either TEBPα (**Fig. 4d**) or TEBPβ (**Fig. 4e**) led to the loss of antibody binding. Thus, both TEBPα and TEBPβ are required for maintaining G-quadruplex DNA structures *in vivo*.

Both TEBPs are required for G-quadruplex formation *in vitro*

To elucidate how TEBPα and TEBPβ are involved in the formation of the G-quadruplex DNA structure at telomeres, we analyzed their *in vitro* DNA binding properties in detail. *Stylonychia* TEBPα and TEBPβ were overexpressed in *E. coli* and purified to homogeneity. A model ciliate telomere consisting of 21 base pairs (bp) of double-stranded DNA and a single-stranded G-overhang ($T_4G_4T_4G_4$) at one 3′ end was constructed from synthetic DNA oligonucleotides. Previous studies have shown that the G-overhang constitutes the binding site for the TEBPs[10,34]. Electrophoretic mobility shift assays (EMSAs) were carried out under conditions aimed to mimic those *in vivo*. From the typical size of a macronucleus (diameter ~25–40 μm and length ~80–120 μm), the approximate number of DNA molecules in a macronucleus (10^8) and Avogadro's constant, we estimated the macronuclear telomere concentration *in vivo* to be >1 μM. Accordingly, the concentration of telomeric DNA in the *in vitro* binding studies presented here was 1 μM. We incubated the model telomeres with increasing concentrations of TEBPα and TEBPβ and analyzed their binding properties by EMSAs in nondenaturing agarose gels (**Fig. 5**). TEBPα bound the G-overhang (**Fig. 5a**), whereas TEBPβ on its own did not (**Fig. 5b**). TEBPβ only bound the model telomere in

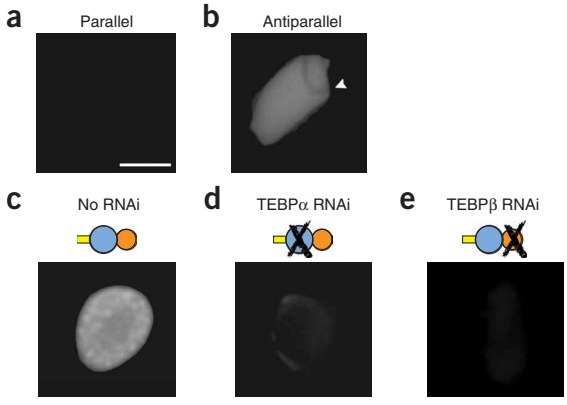

Figure 4 Folding of telomeric G-overhangs into an antiparallel G-quadruplex DNA structure requires both TEBPα and TEBPβ *in vivo*. (**a**,**b**) Staining of *Stylonychia* macronuclei with Sty3, an antibody specific for parallel G-quadruplex DNA structures (**a**), or Sty49, an antibody that detects both parallel and antiparallel G-quadruplex DNA structures (**b**). The results suggest that telomeric G-overhangs adopt only the antiparallel G-quadruplex DNA structure *in vivo*. G-quadruplex DNA structures are absent from the replication band (arrow). Scale bar represents 10 μm. (**c**–**e**) Staining of *Stylonychia* macronuclei with Sty49. Schematics are as in **Figure 2**. (**c**) Telomeric G-overhangs fold into antiparallel G-quadruplex DNA structures before RNAi silencing. (**d**,**e**) Telomeric G-overhangs cannot fold into antiparallel G-quadruplex DNA structures when either TEBPα (**d**) or TEBPβ (**e**) expression is silenced by RNAi.

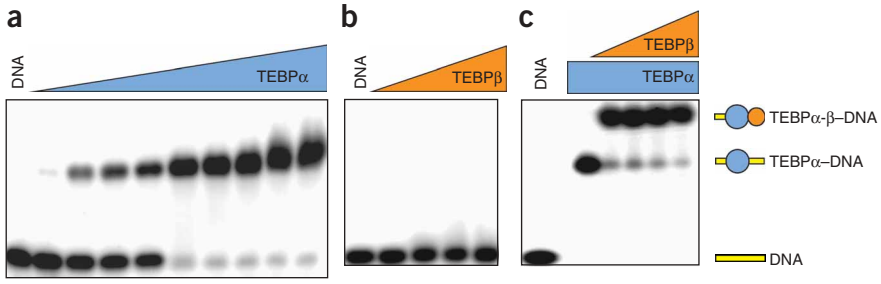

Figure 5 TEBPβ requires TEBPα in order to interact with telomeric DNA *in vitro*. (**a**,**b**) EMSA results after incubation of the model telomere with increasing concentrations of TEBPα (**a**) or TEBPβ (**b**). (**c**) EMSA results after the model telomere–TEBPα complex was titrated with increasing concentrations of TEBPβ. The concentration of DNA was 1 μM and that of the proteins ranged from 0.25–4 μM. Analyses were carried out on a nondenaturing 0.4% (w/v) agarose gel. Blue, TEBPα; orange, TEBPβ. Cartoons, right, mark the migration of each complex and show its components.

the presence of TEBPα (**Fig. 5c**), consistent with previous conclusions for the *Oxytricha nova* TEBPs[34].

Next, we investigated the conformation of the DNA in the TEBPα-β heterodimer. This was done by using the Sty49 antibody to detect the antiparallel G-quadruplex DNA structure *in vivo* and by footprinting. If a G-quadruplex DNA structure was present in a complex, the expectation was that the antibody would bind to it and change the electrophoretic mobility of the complex. Owing to the limiting concentration of the antibody, the telomere DNA concentration in this experiment was 0.1 μM. A band of unique electrophoretic mobility indeed appeared, but only when the telomeric DNA had been bound to the TEBPα-β heterodimer before incubation with the antibody (**Fig. 6a**, lanes 5–8). By contrast, the antibody did not alter the electrophoretic mobility of the telomeric DNA on its own or when incubated with only TEBPβ (data not shown) or only TEBPα (**Fig. 6a**, lane 4). Although the intensity of the antibody-specific band was concentration dependent, it was not possible to reach saturation of binding owing to the limiting concentration of the antibody. The electrophoretic mobility of the band containing the antibody was higher than that of the band containing the TEBPα-TEBPβ–DNA complex (**Fig. 6a**, lanes 5–8), which suggests that a protein was released from the complex upon antibody binding. The most likely explanation is that antibody binding caused displacement of TEBPβ. Whatever the composition of the complex with the antibody is, it does not affect the interpretation that formation of the G-quadruplex DNA structure requires both TEBPα and TEBPβ. These results strongly suggest that both TEBPα and TEBPβ are required to fold the telomeric G-overhang into the G-quadruplex DNA structure that is present *in vivo*.

To further delineate the formation of the antiparallel G-quadruplex DNA structure, TEBPβ lacking the C terminus ($TEBP\beta_{1–230}$) was produced and tested in our binding studies. This experiment was based on two previous biochemical studies[15,35], which had implied that the C terminus of TEBPβ is required for the formation of G-quadruplex DNA structures. The truncated $TEBP\beta_{1–230}$ formed a stable ternary complex with full-length TEBPα and telomeric DNA (**Fig. 6a**, lane 10), but incubation with the antibody did not produce a band of unique electrophoretic mobility (**Fig. 6a**, lane 11). This suggests that the complex with $TEBP\beta_{1–230}$ contains single-stranded DNA, whereas the presence of the full-length TEBPβ results in the formation of the antiparallel G-quadruplex DNA structure. Thus, the C terminus of TEBPβ thus is responsible for formation of the G-quadruplex DNA structure.

To address directly the question of the folding state of the G-overhang in the various reconstituted TEBP–telomeric DNA complexes and to validate the interpretation of our EMSAs, we probed the various complexes with dimethyl sulfate (DMS) (**Fig. 1b**). Whereas DMS specifically methylates non–hydrogen bonded N7 groups on guanines, it cannot react with N7 groups involved in hydrogen bonding (**Fig. 1b**). Consequently, DMS protection provides a reliable test for G-quadruplex DNA structures. We incubated the complexes (**Fig. 6a**) with DMS and analyzed the methylation patterns of the guanines by denaturing gel electrophoresis. The eight guanines present in the telomeric G-overhangs were readily modified in naked DNA in the absence of cations, as expected, but also when the model telomere had been incubated with KCl overnight or with TEBPβ alone (**Fig. 6b**, lanes 2, 3 and

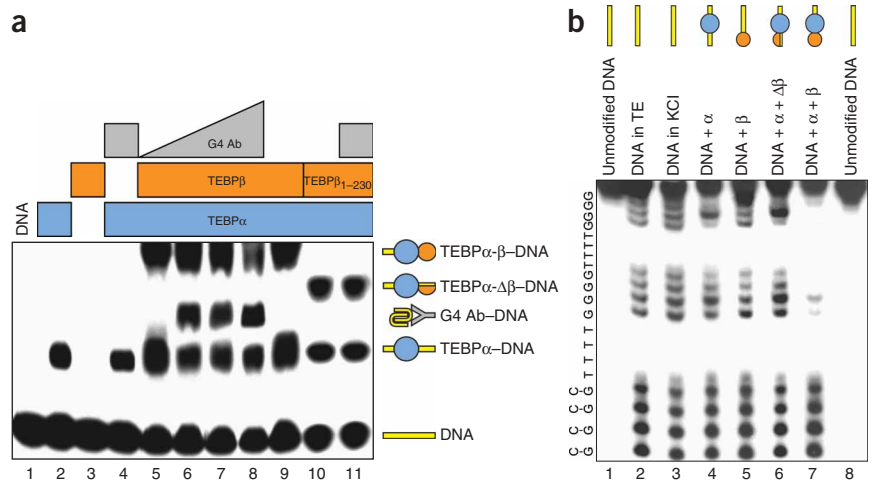

Figure 6 Both TEBPs are required for G-quadruplex DNA formation and the basic C terminus of TEBPβ is essential. (**a**) EMSA results. Proteins included in EMSAs are shown above the lanes. Addition of the sty49 antibody to the G-quadruplex (G4 Ab) results in a complex of altered electrophoretic mobility when the telomeric DNA is bound by the TEBPα-β heterodimer (lanes 6–8). In this experiment the concentration of the telomeric DNA is 0.1 μM because of the limiting concentration of the G-quadruplex antibody. By contrast, the complex with $TEBP\beta_{1–230}$ (Δβ) does not show a band of altered mobility when incubated with the G-quadruplex antibody (lane 11). Analysis was carried out on a 0.4% (w/v) nondenaturing agarose gel. Blue, TEBPα; orange, TEBPβ; gray, G4 Ab. Cartoons, right, mark the migration of each complex and show its components. (**b**) DMS footprinting results. Left, the sequence of the model telomere used in both gel mobility and footprinting experiments. DNA concentration was 1 μM. Buffer conditions and proteins bound to the telomere before DMS probing are shown above each lane (cartoons and coloring as in **a**). Analysis was carried out on a 20% (w/v) denaturing polyacrylamide gel.

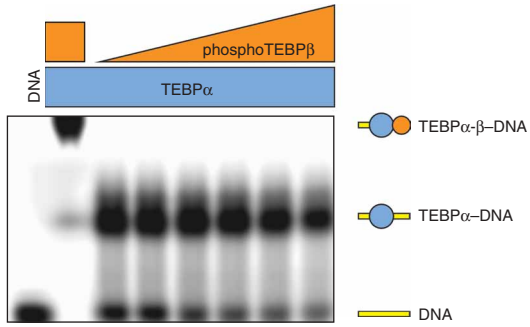

Figure 7 Phosphorylated TEBPβ does not interact with telomeric DNA bound by TEBPα *in vitro*. Lane 1, free DNA; lane 2, control with unphosphorylated TEBPβ; lanes 3–8, titration of TEBPα-bound telomeric DNA with phosphorylated TEBPβ (phosphoTEBPβ) in two-fold dilution steps. The concentrations of DNA and TEBPα were 1 μM each, and the TEBPβ concentration ranged from 0.25–4 μM.

5). Incubation with TEBPα alone or with TEBPα and TEBPβ$_{1–230}$ together led to some protection (**Fig. 6b**, lane 4). This might be expected from the mode of binding observed in the crystal structure of the TEBPα-β heterodimer–DNA complex, in which the bases in the single-stranded G-overhang are buried in a protein cleft[14]. Only in the complex containing both full-length TEBPs were the two tracts of guanines in the G-overhang protected from DMS modification (**Fig. 6b**, lane 7). This provides strong evidence that the G-overhang in this complex is folded into a G-quadruplex DNA structure. In contrast, the G-overhang in the complex with TEBPα-β$_{1–230}$ was accessible to modification, suggesting that it remains in a single-stranded form (**Fig. 6b**, lane 6). Overnight incubation of the model telomere (1 μM) in KCl did not result in the spontaneous formation of a G-quadruplex DNA structure, providing further evidence for the important roles of TEBPα and TEBPβ in modulating the structure of telomeric DNA. Thus, the DMS footprinting data (**Fig. 6b**) are entirely consistent with the results of antibody probing and EMSAs (**Fig. 6a**), and they provide further evidence that both full-length TEBPs are essential for the folding of single-stranded telomeric G-overhangs into G-quadruplex DNA structures. The *in vitro* results pinpoint the different functions of TEBPα and TEBPβ. The role of TEBPα is to bind the G-overhang and recruit TEBPβ, which in turn is responsible for the conversion of the single-stranded G-overhang into a G-quadruplex DNA structure. Moreover, the formation of DNA structure can be attributed to the very basic C terminus of TEBPβ.

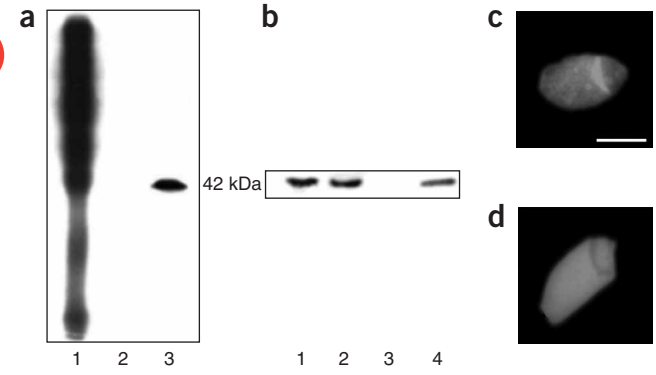

Figure 8 TEBPβ is phosphorylated during S phase, and inhibition of phosphorylation prevents the G-quadruplex DNA structure from being resolved during replication. (**a**) Visualization of nuclear proteins pulse-labeled *in vivo* before and after electroelution. Lane 1, total phosphorylated nuclear proteins during S phase; lane 2, electroeluted phosphorylated nuclear proteins during G_0 phase; lane 3, electroeluted phosphorylated nuclear proteins during S phase (lane 3). (**b**) Western blots of TEBPβ. Lanes 1 and 2, total nuclear proteins during S phase and G_0 phase, respectively; lanes 3 and 4, electroeluted nuclear proteins during G_0 phase and S phase, respectively. (**c**,**d**) *In situ* antibody staining of the G-quadruplex DNA structure in Cdk2-inhibited cells (**c**) and control (**d**). Scale bar represents 10 μm.

TEBPβ phosphorylation regulates G-quadruplex formation

Structural information on the TEBPα-TEBPβ–DNA complex[14,36] and the observation that this complex blocks telomerase activity[37] strongly suggest that the TEBPα-β heterodimer bound to the telomeric DNA end needs to be disrupted for the end-replication machinery to gain access. The cyclin-dependent kinase (Cdk) family of proteins are positive regulators of eukaryotic cell cycle progression. We considered the possibility[38] that phosphorylation of TEBPα or TEBPβ by a Cdk could influence telomere accessibility. A search for potential phosphorylation sites[39] in the amino acid sequences of the *Oxytricha* and *Stylonychia* TEBPs showed that TEBPα lacks a consensus Cdk2 recognition sequence and cannot be phosphorylated *in vitro* by Cdk2 (data not shown). In contrast, TEBPβ contains two closely spaced consensus Cdk2 recognition sequences[38] (**Supplementary Fig. 1** online). Both sites are located in the C terminus of TEBPβ and are conserved in *Oxytricha* and *Stylonychia*. To test the effect of phosphorylation on the binding properties of TEBPβ, it was phosphorylated *in vitro* using Cdk2. EMSA experiments (**Fig. 7**) showed that phosphorylated TEBPβ was no longer able to bind to telomeric DNA bound by TEBPα as in **Figure 5c**. Consequently, phosphorylation of TEBPβ prevents complex formation with TEBPα and the telomeric G-overhang.

We next asked whether TEBPβ is phosphorylated *in vivo* in a cell cycle–dependent manner. *Stylonychia* cells were synchronized[40], pulse-labeled with [γ-^{32}P]ATP and electroeluted at different stages of the cell cycle. Although many proteins are phosphorylated during the S phase (**Fig. 8a**, lane 1), only one phosphorylated protein of molecular weight 42 kDa was electroeluted during DNA replication (**Fig. 8a**, lane 3). This protein could not be electroeluted during other stages of the cell cycle (**Fig. 8a**, lane 2). Western analysis confirmed that the phosphorylated 42-kDa protein was TEBPβ (**Fig. 8b**). To investigate the effect of *in vivo* phosphorylation of TEBPβ on the formation of the G-quadruplex DNA structure, the activity of Cdk2 was inhibited with butyrolactone[41]. As before (**Fig. 4**), the nuclei were stained *in situ* with the Sty49 antibody. The G-quadruplex DNA structure was present in the replication band (**Fig. 8c**), whereas no detectable amount of G-quadruplex DNA in the replication band could be observed in control cells (**Figs. 4** and **8**). Together with the *in vitro* binding data (**Fig. 7**), these results suggest that phosphorylation of TEBPβ during S phase prevents binding of TEBPβ to TEBPα complex or, more likely, that it allows TEBPβ to dissociate from the TEBPα–G-overhang complex. These findings constitute strong evidence that phosphorylation of TEBPβ is required for the unfolding of the G-quadruplex DNA structure during replication *in vivo*.

DISCUSSION

The telomere end-binding proteins TEBPα and TEBPβ bind telomeric G-overhangs in the macronucleus of the ciliate *Stylonychia*. By using RNAi to silence the expression of the two TEBP genes, we have now

been able to characterize their *in vivo* functions in detail. We show that TEBPα is important both for the attachment of telomeres to a subnuclear structure and for the recruitment of TEBPβ to the attachment sites. We also show that antiparallel-type G-quadruplex DNA structure forms at telomeres when they are bound to a subnuclear structure *in vivo*. However, as telomere-telomere interactions remain intact when the TEBP complex is dissociated from the subnuclear structure by high-salt treatment, attachment *per se* seems to be independent from G-quadruplex formation[18]. Silencing of TEBP expression by RNAi shows that formation of the G-quadruplex DNA structure requires both TEBPα and TEBPβ *in vivo*.

In vitro DNA binding and footprinting studies using a model telomere and purified TEBPs further reveal the separate roles of TEBPα and TEBPβ in formation of the G-quadruplex DNA structure. Under our experimental conditions, TEBPα is required first to bind to the telomeric G-overhang and second to recruit TEBPβ to the telomere to form a stable DNA–protein complex. This discovery is only in partial agreement with the previous report that TEBPβ alone can accelerate the formation of G-quadruplex DNA structures *in vitro*[15,35]. TEBPβ lacking the C-terminal domain ($TEBP\beta_{1–230}$) still forms a ternary complex with TEBPα and the G-overhang, but antibody probing and footprinting by DMS did not detect the G-quadruplex DNA structure in the complex. These results show that the C terminus of TEBPβ, which is basic and has sequence homology to the linker histone H1, is essential for promoting the folding of the G-overhang into a G-quadruplex DNA structure. This observation is in agreement with conclusions from previous *in vitro* binding studies[15,35] and also with the crystal structure of the TEBPα-β heterodimer in complex with $G_4T_4G_4$, in which the DNA is in a single-stranded form[14]. In this structure, TEBPβ is truncated at residue 260 and lacks the larger part of the C-terminal domain that we show is responsible for the formation of the G-quadruplex DNA structure.

Evidence for a possible regulation mechanism for G-quadruplex DNA formation comes from our analysis of the phosphorylation states of the TEBPs. Our *in vitro* binding studies show that phosphorylation of TEBPβ blocks interactions with the TEBPα-bound telomeric G-overhang and hence prevents conversion of the single strand into the G-quadruplex DNA structure. The importance of TEBPβ phosphorylation is further substantiated by *in vivo* studies, which show that *Stylonychia* TEBPβ becomes phosphorylated during S phase. We show a direct link between the phosphorylation state of TEBPβ and G-quadruplex DNA formation. Inhibition of phosphorylation during S phase results in the presence of G-quadruplex DNA structure in the replication band, suggesting that phosphorylation of TEBPβ is required for the unfolding of G-quadruplex DNA structure. Notably, the two putative Cdk2 phosphorylation sites are located in the C-terminal domain of TEBPβ, which we have shown is responsible for G-quadruplex DNA formation.

Our results allow us to propose a model for the regulation of G-quadruplex DNA structure formation *in vivo*. We show that *in vivo* the G-quadruplex DNA structure is antiparallel, rather than parallel. This is consistent with the observation that the nanochromosomes of *Stylonychia* macronuclei are joined end to end via their telomeres[18,24], as the most likely structure resulting from the pairing of two $T_4G_4T_4G_4$ overhangs is an antiparallel G-quadruplex[42]. The extensive three-dimensional structural information on the *Oxytricha* TEBPα homodimer and TEBPα-β heterodimer in complex with telomeric DNA[11,14,36] provides insights into how G-quadruplex DNA formation at telomeres might occur. The crystal structure of TEBPα showed that it forms a homodimer, which binds two telomeres and promotes telomere-telomere associations[11]. The DNA in this complex is single stranded, which is consistent with our antibody probing and footprinting data. In the second structure, that of the TEBPα-TEBPβ–DNA complex[14,36], the G-overhang is also bound in an extended and single-stranded form. However, this structure contained a truncated TEBPβ that lacked the C terminus, which our *in vitro* binding studies show is required for G-quadruplex DNA formation. In complex with $TEBP\beta_{1–230}$, the DNA remains in a single-stranded conformation, whereas in complex with full-length TEBPβ, the bound G-overhang adopts G-quadruplex DNA structure. As has been shown here and also suggested elsewhere[15], the highly basic C terminus of TEBPβ seems to act as a chaperone to promote G-quadruplex DNA formation. The discovery that TEBPβ is phosphorylated in a cell cycle–dependent manner provides strong evidence that this protein is responsible for regulating G-quadruplex DNA formation *in vivo*. TEBPβ is phosphorylated during S phase, which is likely to result in dissociation of the TEBPα-β heterodimer. Once this has occurred, the G-quadruplex DNA structure unfolds into a single strand, which would make telomeres accessible for the end-replication machinery. As G-quadruplex DNA structures are very stable under physiological conditions, it remains to be determined how they are resolved *in vivo* in a timely manner.

Could G-quadruplex DNA structures be a general telomere capping structure? Research on telomerase inhibitors has provided indirect support for the presence of G-quadruplex DNA structures at telomeres in human cells. The use of ligands that stabilize G-quadruplexes results in senescence and telomere shortening in telomerase-positive human cell lines[43,44]. G-quadruplex DNA structures have also been implicated in the function of the *Rtel* gene, which is required for telomere elongation in mouse cells[45]. These observations are consistent with the view that G-quadruplex DNA structures may act as caps by making the 3′ overhang inaccessible to telomerase[20] and exonucleases. Our finding, that telomere end-binding proteins control the formation of G-quadruplexes in a cell cycle–dependent manner, indeed suggests that G-quadruplex DNA structures are a core component in telomere capping.

METHODS

Isolation and electroelution of macronuclei. *Stylonychia* macronuclei were isolated and electroeluted essentially according to established protocols[25,30,46]. About 1×10^5 cells were embedded in 1.6% (w/v) low–melting point agarose. The agarose blocks were melted at 65 °C and digested with agarase (Fermentas) 3 h at 42 °C. Nuclei were recovered by centrifugation at 1,000*g* for 5 min, resuspended in 100 µl PBS containing 2% (v/v) formaldehyde and incubated 30 min at room temperature. Nuclei were transferred onto microscopic slides and dried for *in situ* antibody staining and FISH analysis.

***In situ* antibody staining, FISH analysis and western analysis.** These were performed as described in refs. 21,25.

Inhibition of gene expression by RNA interference. To silence TEBPα and TEBPβ, fragments (500 bp) from various regions of the TEBPs were amplified by PCR and cloned into the L4440 vector[47]. The vectors were transfected into RNase III–deficient *E. coli* HT115 cells, and RNAi expression was induced by adding IPTG to a final concentration of 0.4 mM when the cell culture reached an OD_{600} of about 0.4. Specific inhibition of TEBPα or TEBPβ expression was achieved by feeding *Stylonychia* cells heat-inactivated *E. coli* containing the appropriate L4440 vector mixed with *Chlorogonium elongatum*[31]. A strong RNAi effect was observed 4 d after feeding. As a control, cells were fed with *E. coli* containing the L4440 vector without an insert.

Oligonucleotides. Oligonucleotides were synthesized by Sigma-Genosys and purified by denaturing polyacrylamide gel electrophoresis. The oligonucleotides TelG (5′-GCTACACTTGCCAT$_4$G$_4$T$_4$G$_4$T$_4$G$_4$-3′) and TelC (5′-C$_4$A$_4$TGGCAA GTGTAGC-3′) were annealed to form the model telomere with a 16-nt

G-overhang. Oligonucleotide concentrations were estimated from OD_{260} measurements and sequence-specific extinction coefficients.

Protein expression and purification. The genes encoding the full-length *Stylonychia* TEBPα (GenBank accession number AY751782) and TEBPβ and TEBPβ_{1-230} were cloned into a modified Pet30a vector (Novagen) containing an N-terminal 6× His-tag and S-tag followed by a tobacco etch virus (TEV) protease cleavage site. Inserts were verified by sequencing and the plasmids transfected into *E. coli* Rosetta cells (Novagen). Protein expression and purification were carried out essentially as described for the dimerization domains of the human TRF proteins[48]. The purification procedure involved affinity purification using Ni-NTA resin (Qiagen) followed by TEV protease cleavage to remove the 6× His-tag and S-tag. The TEV protease itself was 6× His-tagged, which allowed the cleaved proteins to be purified from the TEV protease and the cleaved N-terminal 6× His-tag and S-tag by rebinding to Ni-NTA resin. Finally, the proteins were purified to homogeneity by gel filtration on a Superdex 200.

Electrophoretic mobility shift assays. DNA was radioactively labeled using [γ-^{32}P]ATP (Amersham) and T4 polynucleotide kinase (New England Biolabs). Unincorporated radiolabel was removed on Bio-Spin P30 columns (Bio-Rad). Labeled DNA (1 μM) was incubated with protein in binding buffer (50 mM Tris/HCl (pH 8.0), 125 mM KCl, 5 mM DTT and 10% (v/v) glycerol) containing 100 μg ml^{-1} BSA (New England Biolabs) and 100 μg ml^{-1} sheared *E. coli* DNA for 12 h at room temperature. Reaction mixtures were analyzed by nondenaturing agarose gel electrophoresis (0.4% (w/v) agarose, 0.25× TB) at 7.5 V cm^{-1} for up to 120 min at 4 °C. Gels were dried onto DE81 paper (Whatman) and scanned using a Typhoon 8600 imaging system (Amersham Pharmacia Biotech).

Antibody mobility shift assays. Radiolabeled DNA (10 nM) was incubated with protein (20 nM) in binding buffer containing 10 μg ml^{-1} BSA and 10 μg ml^{-1} sheared *E. coli* DNA for 12 h at room temperature. The Sty49 antibody was added and the reaction mixtures were incubated 2 h on ice before being analyzed by nondenaturing agarose gel electrophoresis as above.

Dimethyl sulfate footprinting. Radiolabeled DNA was incubated with proteins as described above before footprinting analysis. Methylation was carried out by incubations with 0.2% (v/v) DMS (Sigma) for 10 min at 25 °C. Reactions were terminated by adding 10 μl of a solution containing 1.5 M sodium acetate (pH 9.0), 1.0 M β-mercaptoethanol, 100 μg ml^{-1} sonicated *E. coli* DNA and 10 mM EDTA. An aliquot of each reaction was taken out for immediate analysis by nondenaturing agarose gel electrophoresis and the remainder was purified by phenol-chloroform extraction. The DNA was cleaved with 1 M piperidine, and the piperidine was removed by lyophilization. Samples were analyzed on denaturing 20% (w/v) polyacrylamide (19:1 mono/bis) 8 M urea gels. Gels were autoradiographed and scanned using a Typhoon 8600 imaging system (Amersham Pharmacia Biotech).

***In vitro* and *in vivo* protein phosphorylation.** Purified TEBPβ (4 μM) was incubated with 20 units Cdk2-cycline A (New England Biolabs) for 30 min at 30 °C in a buffer containing 50 mM Tris (pH 7.4), 10 mM β-mercaptoethanol, 10 mM $MgCl_2$, 10 mM γ-glycerol phosphate and 100 μM ATP. For analysis of *in vivo* protein phosphorylation, cells were synchronized[44] and pulse-labeled (2 h) by the addition of 1 μCi ml^{-1} cell culture [γ-^{32}P]ATP (Amersham). Nuclear proteins were separated on 15% (w/v) SDS polyacrylamide gels and autoradiographed. *In vivo* inhibition of Cdk2 activity was achieved by the addition of 10 mM butyrolactone (Acros); *in situ* antibody analysis was performed as above.

Note: Supplementary information is available on the Nature Structural & Molecular Biology website.

ACKNOWLEDGMENTS

This work was supported by a grant from the Deutsche Forschungsgemeinschaft to H.J.L., a European Molecular Biology Organization short-term fellowship to K.P. and a Wenner-Gren Foundations fellowship to T.S. We thank T. Cech (University of Colorado, Boulder, Colorado, USA) for providing antibodies against the TEBP subunits and C. Schaffitzel (Swiss Federal Institute of Technology, Zurich) for providing antibodies against G-quadruplex DNA structures.

COMPETING INTERESTS STATEMENT

The authors declare that they have no competing financial interests.

Published online at http://www.nature.com/nsmb/
Reprints and permissions information is available online at http://npg.nature.com/reprintsandpermissions/

1. Zakian, V.A. Telomeres: beginning to understand the end. *Science* **270**, 1601–1607 (1995).
2. De Lange, T. Protection of mammalian telomeres. *Oncogene* **21**, 532–540 (2002).
3. Jonsson, F. & Lipps, H.J. The biology of telomeres in hypotrichous ciliates. in *Telomerases, Telomeres and Cancer* (eds. Krupp, G. & Parwaresch, R.) 205–222 (Landes Bioscience, Kluwer Academic/Plenum Publishers, Georgetown, Texas, USA, 2002).
4. Klobutcher, L.A., Swanton, M.T., Donini, P. & Prescott, D.M. All gene-sized DNA molecules in four species of hypotrichs have the same terminal sequence and an unusual 3′ terminus. *Proc. Natl. Acad. Sci. USA* **78**, 3015–3019 (1981).
5. Wellinger, R.J., Ethier, K., Labrecque, P. & Zakian, V.A. Evidence for a new step in telomere maintenance. *Cell* **85**, 423–433 (1996).
6. Makarov, V.L., Hirose, Y. & Langmore, J.P. Long G tails at both ends of human chromosomes suggest a C strand degradation mechanism for telomere shortening. *Cell* **88**, 657–666 (1997).
7. Murzin, A.G. OB(oligonucleotide/oligosaccharide binding)-fold: common structural and functional solution for non-homologous sequences. *EMBO J.* **12**, 861–867 (1993).
8. Mitton-Fry, R.M., Anderson, E.M., Hughes, T.R., Lundblad, V. & Wuttke, D.S. Conserved structure for single-stranded telomeric DNA recognition. *Science* **296**, 145–147 (2002).
9. Theobald, D.L. & Wuttke, D.S. Prediction of multiple tandem OB-fold domains in telomere end-binding proteins Pot1 and Cdc13. *Structure (Camb)* **12**, 1877–1879 (2004).
10. Gottschling, D.E. & Zakian, V.A. Telomere proteins: specific recognition and protection of the natural termini of *Oxytricha* macronuclear DNA. *Cell* **47**, 195–205 (1986).
11. Peersen, O.B., Ruggles, J.A. & Schultz, S.C. Dimeric structure of the *Oxytricha nova* telomere end-binding protein alpha-subunit bound to ssDNA. *Nat. Struct. Biol.* **9**, 182–187 (2002).
12. Gray, J.T., Celander, D.W., Price, C.M. & Cech, T.R. Cloning and expression of genes for the *Oxytricha* telomere-binding protein: specific subunit interactions in the telomeric complex. *Cell* **67**, 807–814 (1991).
13. Fang, G. & Cech, T.R. *Oxytricha* telomere-binding protein: DNA-dependent dimerization of the alpha and beta subunits. *Proc. Natl. Acad. Sci. USA* **90**, 6056–6060 (1993).
14. Horvath, M.P., Schweiker, V.L., Bevilacqua, J.M., Ruggles, J.A. & Schultz, S.C. Crystal structure of the *Oxytricha nova* telomere end binding protein complexed with single strand DNA. *Cell* **95**, 963–974 (1998).
15. Fang, G. & Cech, T.R. The beta subunit of *Oxytricha* telomere-binding protein promotes G-quartet formation by telomeric DNA. *Cell* **74**, 875–885 (1993).
16. Sundquist, W.I. & Klug, A. Telomeric DNA dimerizes by formation of guanine tetrads between hairpin loops. *Nature* **342**, 825–829 (1989).
17. Williamson, J.R., Raghuraman, M.K. & Cech, T.R. Monovalent cation-induced structure of telomeric DNA: the G-quartet model. *Cell* **59**, 871–880 (1989).
18. Lipps, H.J. *In vitro* aggregation of the gene-sized DNA molecules of the ciliate *Stylonychia mytilus*. *Proc. Natl. Acad. Sci. USA* **77**, 4104–4107 (1980).
19. Giraldo, R. & Rhodes, D. The yeast telomere-binding protein RAP1 binds to and promotes the formation of DNA quadruplexes in telomeric DNA. *EMBO J.* **13**, 2411–2420 (1994).
20. Zahler, A.M., Williamson, J.R., Cech, T.R. & Prescott, D.M. Inhibition of telomerase by G-quartet DNA structures. *Nature* **350**, 718–720 (1991).
21. Schaffitzel, C. *et al.* *In vitro* generated antibodies specific for telomeric guanine-quadruplex DNA react with *Stylonychia lemnae* macronuclei. *Proc. Natl. Acad. Sci. USA* **98**, 8572–8577 (2001).
22. Meyer, G.F. & Lipps, H.J. The formation of polytene chromosomes during macronuclear development of the hypotrichous ciliate *Stylonychia mytilus*. *Chromosoma* **82**, 309–314 (1981).
23. Murti, K.G. & Prescott, D.M. Topological organization of DNA molecules in the macronucleus of hypotrichous ciliated protozoa. *Chromosome Res.* **10**, 165–173 (2002).
24. Lipps, H.J., Gruissem, W. & Prescott, D.M. Higher order DNA structure in macronuclear chromatin of the hypotrichous ciliate *Oxytricha nova*. *Proc. Natl. Acad. Sci. USA* **79**, 2495–2499 (1982).
25. Postberg, J. *et al.* Association of the telomere-telomere binding protein-complex of hypotrichous ciliates with the nuclear matrix and dissociation during replication. *J. Cell Sci.* **114**, 1861–1866 (2001).
26. de Lange, T. Human telomeres are attached to the nuclear matrix. *EMBO J.* **11**, 717–724 (1992).
27. de Lara, J., Wydner, K.L., Hyland, K.M. & Ward, W.S. Fluorescent *in situ* hybridization of the telomere repeat sequence in hamster sperm nuclear structures. *J. Cell. Biochem.* **53**, 213–221 (1993).

28. Laroche, T., Martin, S.G., Tsai-Pflugfelder, M. & Gasser, S.M. The dynamics of yeast telomeres and silencing proteins through the cell cycle. *J. Struct. Biol.* **129**, 159–174 (2000).
29. Jonsson, F., Postberg, J., Schaffitzel, C. & Lipps, H.J. Organization of the macronuclear gene-sized pieces of stichotrichous ciliates into a higher order structure via telomere-matrix interactions. *Chromosome Res.* **10**, 445–453 (2002).
30. Jackson, D.A., Yuan, J. & Cook, P.R. A gentle method for preparing cyto- and nucleo-skeletons and associated chromatin. *J. Cell Sci.* **90**, 365–378 (1988).
31. Paschka, A.G. *et al.* The use of RNAi to analyze gene function in spirotrichous ciliates. *Eur. J. Protistol.* **39**, 449–454 (2003).
32. Schaffitzel, C., Hanes, J., Jermutus, L. & Pluckthun, A. Ribosome display: an *in vitro* method for selection and evolution of antibodies from libraries. *J. Immunol. Methods* **231**, 119–135 (1999).
33. Lipps, H.J. *et al.* Antibodies against Z DNA react with the macronucleus but not the micronucleus of the hypotrichous ciliate *Stylonychia mytilus*. *Cell* **32**, 435–441 (1983).
34. Fang, G., Gray, J.T. & Cech, T.R. *Oxytricha* telomere-binding protein: separable DNA-binding and dimerization domains of the alpha-subunit. *Genes Dev.* **7**, 870–882 (1993).
35. Fang, G. & Cech, T.R. Characterization of a G-quartet formation reaction promoted by the beta- subunit of the *Oxytricha* telomere-binding protein. *Biochemistry* **32**, 11646–11657 (1993).
36. Horvath, M.P. & Schultz, S.C. DNA G-quartets in a 1.86 A resolution structure of an *Oxytricha nova* telomeric protein-DNA complex. *J. Mol. Biol.* **310**, 367–377 (2001).
37. Froelich-Ammon, S.J., Dickinson, B.A., Bevilacqua, J.M., Schultz, S.C. & Cech, T.R. Modulation of telomerase activity by telomere DNA-binding proteins in *Oxytricha*. *Genes Dev.* **12**, 1504–1514 (1998).
38. Hicke, B. *et al.* Phosphorylation of the *Oxytricha* telomere protein: possible cell cycle regulation. *Nucleic Acids Res.* **23**, 1887–1893 (1995).
39. Obenauer, J.C., Cantley, L.C. & Yaffe, M.B. Scansite 2.0: Proteome-wide prediction of cell signaling interactions using short sequence motifs. *Nucleic Acids Res.* **31**, 3635–3641 (2003).
40. Juranek, S.A., Jönsson, F., Maercker, C. & Lipps, H.J. The telomeres of replicating macronuclear DNA molecules of the ciliate *Stylonychia lemnae*. *Protistology* **1**, 148–151 (2000).
41. Kitagawa, M. *et al.* Butyrolactone I, a selective inhibitor of cdk2 and cdc2 kinase. *Oncogene* **8**, 2425–2432 (1993).
42. Rhodes, D. & Giraldo, R. Telomere structure and function. *Curr. Opin. Struct. Biol.* **5**, 311–322 (1995).
43. Riou, J.F. *et al.* Cell senescence and telomere shortening induced by a new series of specific G-quadruplex DNA ligands. *Proc. Natl. Acad. Sci. USA* **99**, 2672–2677 (2002).
44. Rezler, E.M., Bearss, D.J. & Hurley, L.H. Telomeres and telomerases as drug targets. *Curr. Opin. Pharmacol.* **2**, 415–423 (2002).
45. Ding, H. *et al.* Regulation of murine telomere length by Rtel: an essential gene encoding a helicase-like protein. *Cell* **117**, 873–886 (2004).
46. Ammermann, D., Steinbruck, G., von Berger, L. & Hennig, W. The development of the macronucleus in the ciliated protozoan *Stylonychia mytilus*. *Chromosoma* **45**, 401–429 (1974).
47. Timmons, L. & Fire, A. Specific interference by ingested dsRNA. *Nature* **395**, 854 (1998).
48. Fairall, L., Chapman, L., Moss, H., de Lange, T. & Rhodes, D. Structure of the TRFH dimerization domain of the human telomeric proteins TRF and TRF2. *Mol. Cell* **8**, 351–361 (2001).